Conformer-Selective Photoelectron Circular Dichroism

Etienne Rouquet, Jennifer Dupont, Valeria Lepere, Gustavo Garcia, Laurent Nahon, Anne Zehnacker

Conformer-Selective Photoelectron Circular Dichroism

Etienne Rouquet,[a,b] Jennifer Dupont,[a] Valéria Lepère,[a] Gustavo A. Garcia,[b] Laurent Nahon,[b] and Anne Zehnacker[a]*

[a] E. Rouquet, Dr. J. Dupont, Dr. V. Lepère, Dr. A. Zehnacker
Institut des Sciences Moléculaires d'Orsay (ISMO), CNRS, Université Paris-Saclay
F 91405 Orsay, France
E-mail: anne.zehnacker-rentien@universite-paris-saclay.fr
[b] E. Rouquet, Dr. G. A. Garcia, Dr. L. Nahon,
Synchrotron Soleil, L'Orme des Merisiers
St. Aubin BP48, F-91192 Gif sur Yvette, France

Abstract: Conformational flexibility and chirality both play a key role in molecular recognition. It is therefore very useful to develop spectroscopic methods that simultaneously probe both properties. It has been theoretically predicted that photoelectron circular dichroism (PECD) should be very sensitive to conformational isomerism. However, experimental proof has been less forthcoming and only exists for a very few favorable cases. Here, we present a new PECD scheme based on resonance-enhanced two-photon ionization (RE2PI) using UV/Vis nanosecond laser excitations. The spectral resolution obtained thereby guarantees conformer-selectivity by inducing resonant conformer-specific $\pi\pi^* S_1 \leftarrow S_0$ transitions. We apply this experimental scheme to the study of chiral 1-indanol, which exists in two conformers linked by a ring inversion and defined by the position of the hydroxyl group, namely axial and equatorial. We show that the PECD of the equatorial and axial forms considerably differ in sign, magnitude and shape. We also discuss the influence of the total ionization energy, vibronic excitation of intermediate and final states, and relative polarization of the excitation and ionization lasers. Conformer-specificity adds a new dimension to the applications of PECD in analytical chemistry addressing now the general case of floppy systems.

Introduction

Molecular recognition is responsible for the selectivity of numerous biochemical reactions; it also finds applications in analytical chemistry, for example in chromatography where it dictates which molecule will be retained on the column and which won't. Molecular recognition is influenced by several factors, among which chirality and conformational flexibility play a decisive role. This has prompted the development of spectroscopic methods that are sensitive to both of these molecular properties. This is the case of chiroptical spectroscopy, which in addition to its ability to determine absolute configurations of chiral molecules with the aid of quantum chemical calculations, is very sensitive to conformational isomerism. Electronic circular dichroism (ECD) is for example routinely used for assessing the secondary structure composition of proteins.[1-2] In the IR range, vibrational circular dichroism (VCD) also provides an exquisite probe of conformation and its modification upon molecular interaction.[3-6] Despite their sensitivity to conformation, these methods are not conformer-selective, because they rest on direct absorption in the condensed phase where multiple conformers coexist and absorb in the same energy range. The obtained spectrum therefore contains the contribution of all the structures populated at the sample temperature. In addition, solvent effects need to be considered, limiting the amount of information recovered by comparison with theoretical methods.

In contrast, electronic or vibrational spectroscopy experiments conducted in the gas-phase reach selectivity because of the narrow bandwidth in absorption, which allows selecting a given conformer. For more than two decades, so-called double resonance experiments have been developed under supersonic jet conditions or in a cryogenic ion trap; they now reach conformer selectivity even in complex molecular systems.[7-9] However, these methods are blind to chirality. Various strategies have been explored to add chiral sensitivity, such as complexation with another chiral molecule,[10-11] and methods resting on nonlinear resonant phase-sensitive microwave spectroscopy,[12] or the use of circularly polarized light. Direct observation of conformer-selective ECD has been recently reported, which clearly evidenced its sensitivity to molecular conformation.[13-14] However, the weak chiroptical asymmetries inherent to ECD, arising from the simultaneous variation of electric and magnetic transition moments, make these gas phase measurements especially challenging.

In this work we propose an alternative method based on incorporating conformer-selectivity to the well-known photoelectron circular dichroism (PECD) effect. PECD is defined as a forward-backward asymmetry in the photoelectron angular distribution after ionization of pure enantiomers by a circularly polarized light (CPL). As a differential effect, PECD is allowed in the electric dipole approximation, leading to orders of magnitude

more intense asymmetries than ECD, up to almost 40%,[15] making it very suitable for the study of chirality in solvent-free dilute matter. PECD is sensitive to the initial orbital from which the photoelectron is ejected, but also to the final state, and therefore to structural[16] and conformational isomerism.[17-20] This structural sensitivity arises from the fact that PECD is based on the photoelectron scattering off the chiral potential of the cation, which encodes both chirality and conformational information.[21-23]

So far, most PECD studies on floppy systems, either in the valence[18-19, 24-32] or in the core shell,[33-34] have been carried out by one-photon ionization PECD, on samples presenting a mixture of conformations whose population is a priori governed by a Boltzmann distribution, the corresponding experimental global PECD being then reproduced by a conformer Boltzmann-average of individually-calculated PECD. In this case the only "control" of the conformer distribution is the temperature and no conformer selectivity can be achieved. In rare cases however, the PECD of conformational isomers can be obtained separately, for example when the difference between the ionization energies of two conformers is large enough to separate them in the photoelectron spectrum (PES), as exemplified by the amino acid proline.[19] Another favorable situation occurs when the isomer ratio can be controlled by changing the experimental conditions, as recently demonstrated in the case of 1-indanol.[20]

Alternative schemes to one-photon ionization consist in non-resonant multiphoton ionization based on femtosecond table-top laser excitation as introduced a decade ago,[35-36] but their intrinsic large spectral bandwidth precludes conformation selection. In practice, the applicability and performances of fs laser-based PECD have been mainly demonstrated in rigid model systems.[37-41] Overall, both ionization schemes result in the undifferentiated ionization of all the conformers of a flexible molecule.

Schemes based upon nanosecond resonance-enhanced multiphoton ionization (REMPI), with intrinsic high resolution capabilities have also been reported recently.[42-43] The paradigm fenchone and camphor molecules have been studied by a 2+1 REMPI process. Successful resonant ionization of these structural isomers via distinct vibrational levels of the 3s Rydberg state suggest that conformer-specific PECD measurements are at reach. Here we demonstrate in the case of 1-indanol that the ns-REMPI scheme makes conformer-selective PECD possible. The experimental scheme is summarized in Figure 1 and the experimental details are given in the supplementary information (SI). Briefly, the experiment rests on resonance-enhanced two photon ionization (RE2PI) of the molecule of interest cooled down in a supersonic expansion. Mass-resolved $S_1 \leftarrow S_0$ electronic spectra are obtained using one-color resonance-enhanced two-photon ionization (RE2PI) as reported previously.[44]. When several conformers coexist in the supersonic expansion, they display slightly different $S_1 \leftarrow S_0$ transition energies. This resonance condition allows conformer selection. Ionization of the selected conformer happens via absorption of a second photon, provided either by the same laser pulse or by a second laser. The electrons produced thereby are extracted and accelerated by a series of grid-less electrodes to a position-sensitive detector consisting in microchannel plates, a phosphor screen and a camera, yielding photoelectron velocity map images that are further processed to retrieve the photoelectron and PECD spectra.

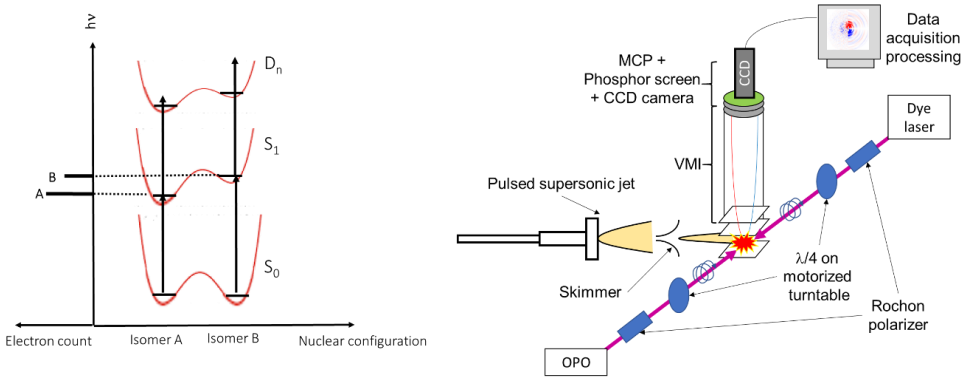

Figure 1. a) Principle of the REMPI scheme used for recording conformer-selective PECD. For the sake of simplicity, the two conformers have been chosen isoenergetic, but the scheme is general. The conformer selectivity is guaranteed by the $S_1 \leftarrow S_0$ transition as shown on the left of the scheme. b) Schematic view of the experimental set-up (see text and experimental details in the SI).

1-indanol is a good candidate since its conformational landscape has been widely studied under supersonic expansion conditions, by laser-induced fluorescence, RE2PI, and IR-UV double resonance vibrational spectroscopy.[45-48] Its structure has been

confirmed by high resolution spectroscopy.[49-50] Moreover, It was used as an example to characterize enantiomer-specific state transfer.[51]

This aromatic molecule, shown in Figure 2a, exists in two conformers related by the five-member ring inversion (also called puckering motion). The most stable conformer, called equatorial in what follows and denoted as I_{eq}, has the hydroxyl group in pseudo equatorial position while it is in pseudo axial position for the less stable form, called axial and denoted as II_{ax}, with an interconversion barrier for the $II_{ax} \rightarrow I_{eq}$ isomerization calculated at 3 kJ mol^{-1}.[46] The geometries of the conformers are given in Tables S1 and S2 of the SI. The I_{eq} / II_{ax} ratio depends on the cooling conditions of the supersonic expansion, which can be controlled by the carrier gas used. In argon, efficient relaxation results in the presence of the most stable equatorial conformer only. In helium, relaxation is less efficient and each conformer is trapped in its own potential well, resulting in an I_{eq} / II_{ax} ratio of 3.

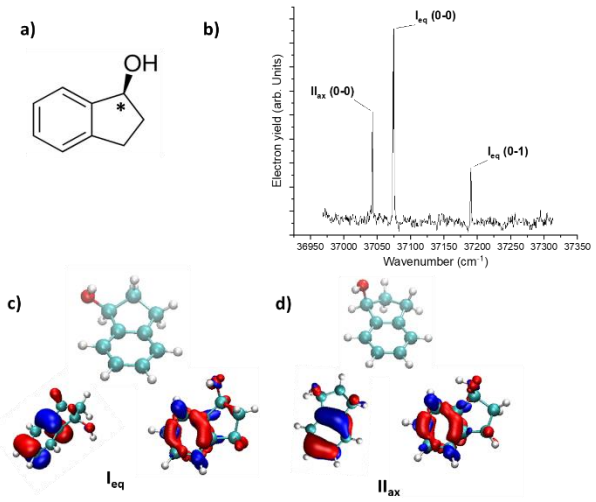

Figure 2. a) Schematic (*S*)-(+)-1-indanol structure. b) $S_1 \leftarrow S_0$ spectrum obtained by monitoring the total number of electrons as a function of the laser wavenumber. The transitions located at 37043, 37075 and 37191 cm^{-1} correspond to the transition origin (0-0) of II_{ax} and I_{eq}, and the vibronic band (0-1) of I_{eq} assigned to the excitation of the ring puckering, respectively. c) Equatorial conformer (I_{eq}) together with the electron density of the highest occupied orbital (HOMO) calculated at the MP2/6-31G++(d,p) level (left) and the electron density difference between the electronic ground state S_0 and the electronic excited state S_1 (right) calculated at the TD-DFT B3LYP-D3BJ/6-311++G(d,p) level. d) Same for the axial conformer (II_{ax}). The orbital energies calculated at the OVGF/cc-pVTZ level using the MP2 geometries are 8.83 eV for I_{eq} and II_{ax} alike.

The valence PECD using one VUV photon ionization dramatically depends upon the carrier gas; in particular the HOMO orbital shows PECD opposite in sign in helium and in argon for an ionization energy of 11 eV.[20] These results prove unambiguously that I_{eq} and II_{ax} have PECD that differ in magnitude and sign. They prompted the conformer-selective PECD study reported here, which rests on a ns REMPI scheme with vibrational resolution. In this ionization scheme, the resonance with a $\pi\pi^*$ $S_1 \leftarrow S_0$ transition ensures conformer selectivity. We shall first present the PECD spectra resulting from the ionization of the $S_1 \leftarrow S_0$ transition origin of each conformer. We shall then discuss the role of vibronic excitation in the S_1 state, that of the total ionization energy, and that of the relative polarization of the excitation and ionization lasers.

Results and Discussion

The photoionization angular distribution function $I^{\{p\}}(\theta)$ is written as a function of θ, the angle of electron emission relative to the light propagation axis, as the sum given in Equation (1). P_n is the Legendre polynomial of degree n, with n being the number of photons involved in the ionization process. In our two-photon case, the sum stops at i=4.

$$I^{\{p\}}(\theta) = \frac{I_{tot}}{4\pi}\left(1 + \sum_{i=1}^{i=2n} b_i^{\{p\}} P_i(cos\theta)\right) \qquad (1)$$

p defines the light polarization, with p= 0, +1, and -1 for linear, left- and right- handed circular polarization, respectively. The isotropic term is the photoelectron spectrum (PES). The odd terms of this equation, b_1, b_3, vanish for linear polarization or non-chiral molecules, in contrast to the even terms. For chiral molecules, $b_1^{\{1\}} = -b_1^{\{-1\}}$ and $b_3^{\{1\}} = -b_3^{\{-1\}}$ so that opposite effects are observed for right and left CPL. Like all chiroptical spectroscopy measurements, the PECD is expected to be opposite in sign for opposite enantiomers. The PECD is defined as the relative difference in electron counts through the backward and forward hemispheres according to Lehmann *et al*.[36] For our two-photon case, this difference can be expressed as:

$$PECD = 2b_1^{\{1\}} - \frac{1}{2}b_3^{\{1\}} \qquad (2)$$

Note that, contrary to the one-photon process, the maximum absolute difference in the two-photon case is not found at exactly the forward/backward direction if $b_3 \neq 0$, but at an angle θ defined by: $\cos^2\theta_{max} = 0.2 - \frac{2b_1}{15b_3}$.[36] Figure 2b shows the one-color two-photon $S_1 \leftarrow S_0$ spectrum obtained by monitoring the total electron current as a function of the laser wavelength. It is identical to that obtained by monitoring the (*S*)-(+)-1-indanol ions at *m/z* 134, which shows that only the (*S*)-(+)-1-indanol monomer is ionized in our experimental conditions.[46] The same spectrum using a two-color scheme, fixing the ionization laser at σ_2 = 40000 cm^{-1} and

scanning the excitation laser σ_1 is shown in Figure S1 of the Supplementary Information. The PECD spectra have been recorded by probing the different bands observed in the spectrum shown in Figure 2, using one- or two-color two-photon ionizing schemes.

One-color two-photon ionization scheme

a) Excitation of the transition origin:

The ionization wavelength was first set on the transitions located at 37075 and 37043 cm^{-1}, assigned to the $S_1 \leftarrow S_0$ transition origin of the I_{eq} and II_{ax} conformers, respectively. These excitation energies correspond to almost identical ionization energies (9.1976 vs. 9.1897 eV), therefore quasi-identical electron kinetic energies. Although PECD is known to depend on electron kinetic energy, this is typically over eVs. The present 8 meV difference in ionization energy cannot be responsible for any PECD difference. The PECD spectra measured thereby are shown in Figure 3, together with the PES. As noted in a previous one-photon ionization study,[20] the ionization thresholds and more generally the PES are identical for I_{eq} and II_{ax}. In contrast, the PECD as a function of the photon energy are strikingly different, both in sign, magnitude and shape for the I_{eq} and II_{ax} conformers of 1-indanol, providing a first direct evidence of conformer-selective PECD. For each of them, a clear asymmetry is measured at this ionization energy, with the expected specular relation between the *(R)* and *(S)* enantiomers showing the quality of the data while, as expected, the PECD of racemic 1-indanol is overall zero (see Figure S2 of the SI).

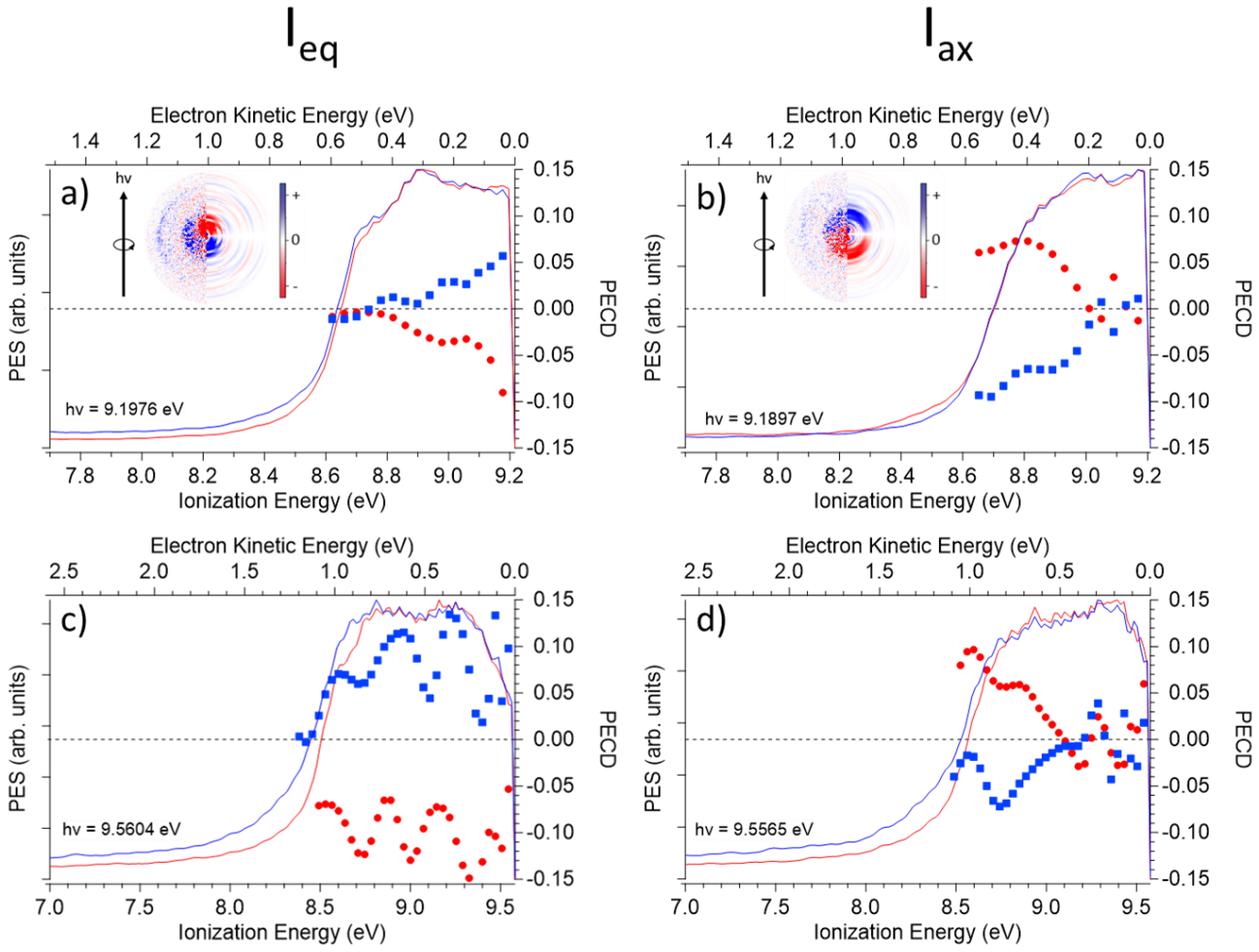

Figure 3. a) Photoelectron spectra (full line) and PECD (squares) for the two enantiomers of 1-indanol excited at the equatorial transition origin at 37075 cm^{-1} in a 1C-R2PI ionization scheme (total ionization energy of 9.1976 eV). b) Same for the axial conformer excited at its transition origin at 37043 cm^{-1} (total ionization energy of 9.1897 eV). The inserts are the LCP-RCP raw (left) and Abel inverted (right) electron images for both conformers.

c) Photoelectron spectra (full line) and PECD (squares) for the two enantiomers of 1-indanol excited at the equatorial transition origin at 37075 cm^{-1} in a 2-C-R2PI ionization scheme. The $S_1 \leftarrow S_0$ laser is tuned to the 0-0 transition of the equatorial conformer and the wavenumber of the ionizing laser is 40000 cm^{-1}. d) Same for the axial conformer, with the $S_1 \leftarrow S_0$ laser tuned to the 0-0 transition of the axial conformer. The *(R)* enantiomer is shown in blue and the *(S)* in red.

The PECD spectrum of *(R)*-I_{eq} is almost zero at the ionization onset then increases to a positive value of ~7%, while the PECD spectrum of *(R)*-II_{ax} is strongly negative at the threshold (-10%), then decreases and oscillates around zero. Note that at this ionization energy, only the HOMO orbital can be ionized. Its iso-density contour (see Figure 2c,d) is very similar for the two conformers and corresponds to a HOMO orbital localized on the aromatic ring, i.e. relatively far from the chiral center.[20] Because the HOMO orbitals are the same for the two conformers, the conformer sensitivity observed in the one-photon PECD of 1-indanol was explained in terms of the effect of the scattering potential. The ionization scheme is more complicated here as the intermediate S_1 state may play a role. However, the state populated by the $S_1 \leftarrow S_0$ transition is identical too for the two conformers, as shown by the electron density difference shown between the S_0 and S_1 states (see Figure 2c,d). This unambiguously shows that the strong sensitivity of the PECD to conformation results from the scattering potential and, in this case, not from the initial orbital of the ground or electronic excited state neutral species.

b) Vibronic effects: excitation of the puckering motion:

As mentioned above, the two conformers of 1-indanol are related by the 5-member-ring puckering motion (see Tables S3 and S4 in the SI for the description of the normal modes). It is therefore interesting to know whether exciting this motion in the S_1 state has an influence on PECD. In other words, does the PECD of the equatorial conformer become more “axial-like” when one excites the motion that allows the molecule to evolve from equatorial to axial? The PECD obtained when exciting the 0-0 + 116 cm^{-1} band of I_{eq}, assigned to one quantum of the puckering motion,[48] is compared to that obtained after excitation of the 0-0 transition in Figure 4. The ionization energies are similar, 9.2264 eV for the former vs. 9.1976 eV for the latter. Again, the PECD spectra show excellent specular relation for the two enantiomers. Excitation of one quantum of the puckering motion in S_1 slightly modifies the shape of the PECD spectrum. For low values of the electron kinetic energy, the asymmetry factor is identical to that obtained when exciting the 0-0 transition. However, the shape changes for electron kinetic energies above 0.2 eV. There, the PECD was close to zero when exciting the 0-0 transition, while excitation of the vibronic band results in oscillations with a ~0.2 eV period in electron kinetic energy. The period of these oscillations might correspond to a 1385 cm^{-1} vibrational mode calculated at the B3LYP-D3BJ/6-311++G(d,p) level in the ion. This mode is described as the coupled C*H and OH bending motions that are precisely located on the asymmetric carbon substituents, where the geometry change happens between the neutral and the ion.[20]

Although a quantitative explanation would require theoretical calculations that are beyond the scope of this article,[52] this vibrationally-dependent PECD may correspond, in our opinion, to a breakdown of the Franck-Condon approximation, as previously observed in the case of other chiral systems such as methyloxirane or bicyclic monoterpene. [15, 53] The bending mode mentioned above involves motion of the very same atoms that are involved in the puckering motion (see Tables S3 and S4 in the SI). The two modes might be coupled, which would explain the influence of the excitation of a vibronic band on the electron–nuclei coupling accompanying the ionization. We probably have here an interplay between vibration-dependent PECD in the final state (cation) as already observed [15, 53] with vibration-dependent PECD in the excited intermediate state of the neutral molecule as reported by Comby *et al.*[39] In the latter study, various vibrational states are populated after ultra-fast intramolecular energy redistribution prior to ionization. In contrast, in the ionization scheme presented here, a specific vibronic state is directly excited.

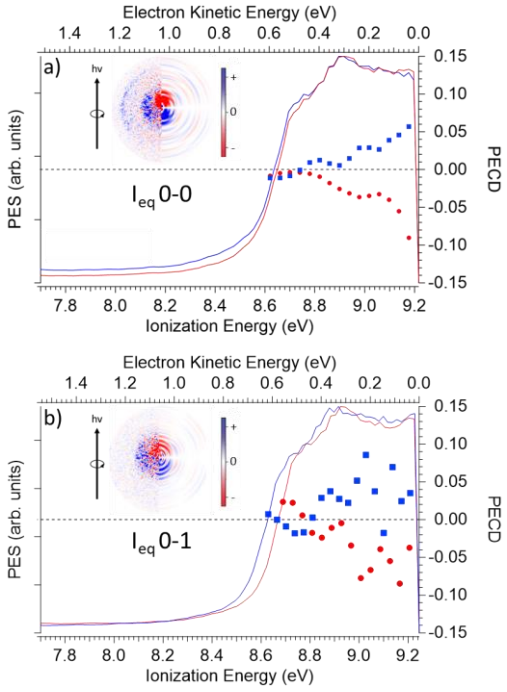

Figure 4: a) Photoelectron spectra (full line) and PECD (squares) for the two enantiomers of 1-indanol excited at the equatorial transition origin (I_{eq} 0-0) at 37075 cm^{-1} (total ionization energy of 9.1976 eV). b) Same for the same equatorial conformer excited at the vibronic transition at 37191 cm^{-1} (total ionization energy of 9.2264 eV). The *(R)* enantiomer is shown in blue and the *(S)* in red. The inserts are the LCP-RCP raw (left) and Abel inverted (right) electron images for both transitions.

Two-color two-photon ionization scheme

a) Effect of the total ionization energy (kinetic energy of the electron):

As a preliminary to these experiments, we chose the polarization of the ionizing laser and optimized its alignment so as to obtain a PECD identical to that shown in Figure 3a when its wavelength is fixed at the transition origin of I_{eq}. The polarization of the laser inducing the $S_1 \leftarrow S_0$ was kept the same as before. Then, the two-color PECD spectra are recorded by setting the laser inducing the $S_1 \leftarrow S_0$ on the I_{eq} or II_{ax} 0-0 transition and fixing the wavenumber of the ionizing laser at a value above the 0-0 transition energy, at 40000 cm^{-1}. The ionization total energy is thus 9.5604 and 9.5565 eV for I_{eq} and II_{ax}, respectively. The two-color PECD spectra are shown in Figure 3, together with the one-color PECD. For the II_{ax} conformer, the two spectra look similar, with a comparable PECD level. Altogether, there is no strong influence of the electron kinetic energy in this energy range. The differences are more marked for the I_{eq} conformer. The PECD recorded at 9.5604 eV is indeed more intense than at 9.1897, reaching a level of ~15 %. Moreover, it exhibits some quite striking oscillations at 9.5604 eV. Although one cannot completely exclude some spurious systematic errors linked to the alignment of the two laser beams in the case of the 2-color scheme, there is still a satisfactory mirror-image relation between the PECD of the two enantiomers. The difference between the PECD at 9.5604 and 9.1897 eV may result from the fact that, for a given final-state cation, PECD depends on the kinetic energy of the outgoing electron, as commonly observed in one-photon PECD experiments. [21, 54] Part of the differences could also arise from vibrational effects or from the fact that the HOMO-1 orbital can be ionized at this total ionization energy, which might modify the shape of the PECD.

b) Polarization and alignment effects.

The question arises as to the role of the polarization of the two lasers, the one that induces the $S_1 \leftarrow S_0$ transition and the one that ionizes the system. To do so, we have applied different polarization schemes. The first idea that would come into mind is to use a linear-circular scheme, as used in time-resolved PECD experiments.[55] However, Abel inversion of the recorded 2D images used to retrieve the 3D distribution of the electrons is restricted to experimental geometries that maintain cylindrical symmetry. Two counter propagating lasers with circular and linear polarization do not obey this condition. Instead, we have used two counter-propagating lasers with CPLs of identical or opposite handedness. Figure 5 shows the result obtained when exciting the transition origin of the equatorial or axial conformer of the *(R)* enantiomer. Changing the relative helicity of the ionizing light results in a quasi-inversion of the PECD signal, which shows that the polarization of the ionizing laser is the key factor for the observed PECD, and that the alignment effect of the intermediate state has here a negligible effect. In the classical approximation limit, it is commonly admitted that rotational dephasing progressively destroys the excited state alignment prior to ionization, in a two-photon process. This is in particular true in the experiments reported here where the temporal resolution of the laser is of the order of 10 ns, which allows full rotational dephasing for molecules of the size of 1-indanol. However, it has been shown that including quantum effects can result in some alignment effects in RE2PI ionization with linear polarized nanosecond lasers.[56] Alignment was observed also in IR-UV double resonance experiments and allowed using polarization schemes to determine the orientation of the vibrational transition moment of simple molecules.[57] The effect vanishes when using a CPL, at least for achiral molecules, because the CPL can be described as a superposition of linear polarization whose contributions cancel out.[56, 58] Still, anisotropic electronic circular dichroism (ECD) has been suggested from the rotational contour dependence of the ECD.[59]

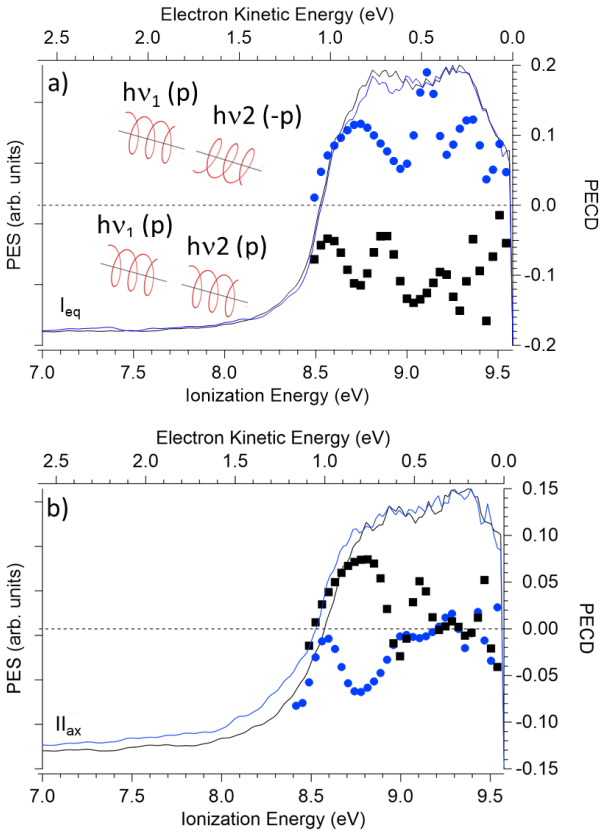

Figure 5: a) Two-color photoelectron spectra (full line) and PECD (squares) for *(R)-(-)*-1-indanol excited at the equatorial (I_{eq}) transition origin at 37075 cm^{-1}. The energy of the ionizing laser is 40000 cm^{-1}. b) Same for the axial conformer (II_{ax}) excited at its transition origin at 37043 cm^{-1}. The polarization of the lasers is given by p, with |p|=1 defining CPL. Parallel and antiparallel CPL are defined by opposite or identical signs of p for $h\nu_1$ and $h\nu_2$ and is shown in black or blue, respectively.

This body of results suggested that alignment effects could also intervene in the experiments described here, which would

manifest themselves by the appearance of a non-zero b_3 term in the definition of PECD.[60] To assess this hypothesis, we have plotted separately the asymmetry parameter $2b_1$-$0.5b_3$ and the $2b_1$ term in Figure S3. There is no difference between the two plots, which shows that no alignment effects intervene in this system. The decisive role of the sole ionizing laser polarization and the fact that b_3 is close to zero both confirm that no alignment effect exists in the S_1 state. In this case, using a linear polarization for the excitation laser should yield the same PECD as a circular polarization. This is indeed the case, as shown in Figure S4. Should this absence of alignment in the S_1 state be a general feature of ns REMPI PECD, besides requiring one CPL laser source only, it would also facilitate the theoretical treatment of PECD with a simpler one-photon approach on randomly-oriented species.

Conclusion

We have measured conformer-specific PECD of the two puckering conformers of 1-indanol for the HOMO orbital thanks to a REMPI scheme using a resonance with the first electronic state populated via a ns laser excitation scheme. The findings obtained in an energy range comprised between 0.6 and 1 eV above the ionization threshold confirm the results of one-photon ionization for the HOMO orbital, that the I_{eq} and II_{ax} conformers display PECD of opposite sign.[20] Their PECD also differ in magnitude, that of II_{ax} being stronger. For the I_{eq} conformer, the PECD shows an energy dependence in the 9.1 - 9.6 eV energy range, which is much less marked for the II_{ax} conformer. The shape of the PECD suggests non-Franck-Condon behavior, an effect reinforced by the excitation of the puckering motion in S_1. Moreover, the negligible value of the b_3 parameter and the fact that the polarization of the excitation laser does not influence the PECD show the absence of alignment in the S_1 state in ns laser experiments.

This first example of conformer-specific PECD, obtained by using a REMPI scheme, has both fundamental and applied implications. First, it adds a new dimension in the interplay between experiment and theory, providing a stringent test of PECD theoretical models based upon an individual conformer-to-conformer basis, instead of a single Boltzmann average of conformer contributions. Conversely, PECD calculations add another observable to study chiral systems where flexibility and therefore conformation is critical, such as in medium sized chiral complexes that act as models of chiral recognition in biological environments.[9, 61-63] Besides, laser-based PECD has been suggested by several groups as being potentially a powerful in situ gas-phase analytical tool allowing the retrieving of enantiomeric excesses (ee),[64-66] possibly in a mixture, which may additionally be separated by coincidence mass spectrometry,[67] by their spectroscopy[43] or their sensitivity to ellipticity.[68] In this context, conformer-selection could increase the sensitivity of ee measurements by selecting the conformer presenting the highest PECD magnitude instead of a mixture of conformations whose average PECD contributions can quickly cancel out with quick oscillations and sign changes (see for instance[19, 29]). This is especially useful when dealing with room temperature samples or in even higher temperature media, such as encountered for instance in combustion processes involving chiral biofuels, for which many conformers with a few kJ mol^{-1} energy separation are populated. Additionally, identification and characterization of individual conformers is interesting since different conformations might present different reactivity.[69] Finally, note that the use of ns laser schemes allows disentangling a mixture of molecules via their spectral fingerprints as demonstrated in a PECD context by Ranecky et al.[43] Spectral fingerprints could be used for analyzing enantiomeric excess by complexation with another chiral molecule, as demonstrated before, especially in the case of complex systems for which the vibrational spectroscopy results are ambiguous.[61, 63, 70-80] However, this method requires formation of a complex which may be a limiting factor in terms of sensitivity and signal detection, in contrast to PECD that can distinguish the enantiomers of bare chiral molecules. The possibility of distinguishing solvent-free molecules and complexes as well as their conformers makes ns-REMPI PECD an ideal tool for chiral analytical chemistry on the general case of floppy systems.

Acknowledgements

AZ and LN thank the financial support of the projects CONF-PECD and FLEX-PECD by the program “Investissements d’Avenir LabEx PALM” (ANR-10-LABX-0039-PALM). We thank Dr. Lionel Poisson for helpful discussions and Julien Vincent for technical support.

Keywords: Chirality • Photoelectron Circular Dichroism • Photoionization • Velocity Map Imaging • Conformer-specific spectroscopy

[1] N. Berova, L. Di Bari, G. Pescitelli, *Chemical Society Reviews* **2007**, *36*, 914-931.
[2] G. R. Jones, D. T. Clarke, *Faraday Discussions* **2004**, *126*, 223-236.
[3] T. A. Keiderling, *Chemical Reviews* **2020**, *120*, 3381-3419.
[4] L. Weirich, G. Tusha, E. Engelage, L. V. Schaefer, C. Merten, *Physical Chemistry Chemical Physics* **2022**, *24*, 11721-11728.
[5] K. Le Barbu-Debus, J. Bowles, S. Jähnigen, C. Clavaguéra, F. Calvo, R. Vuilleumier, A. Zehnacker, *Physical Chemistry Chemical Physics* **2020**, *22*, 26047-26068.

[6] M. Krupova, J. Kessler, P. Bour, *ChemPhysChem* **2021**, *22*, 83-91.

[7] J. T. Lawler, C. P. Harrilal, A. F. DeBlase, E. L. Sibert, III, S. A. McLuckey, T. S. Zwier, *Physical Chemistry Chemical Physics* **2022**, *24*, 2095-2109.

[8] D. Liu, J.-X. Bardaud, Z. Imani, S. Robin, E. Gloaguen, V. Brenner, D. J. Aitken, M. Mons, *Molecules* **2023**, *28*.

[9] M. Tamura, T. Sekiguchi, S.-I. Ishiuchi, A. Zehnacker-Rentien, M. Fujii, *The journal of physical chemistry letters* **2019**, 2470-2474.

[10] A. Zehnacker, *International Reviews in Physical Chemistry* **2014**, *33*, 151-207.

[11] A. Zehnacker, M. A. Suhm, *Angewandte Chemie-International Edition* **2008**, *47*, 6970-6992.

[12] V. A. Shubert, D. Schmitz, D. Patterson, J. M. Doyle, M. Schnell, *Angewandte Chemie-International Edition* **2014**, *53*, 1152-1155.

[13] A. Hong, C. M. Choi, H. J. Eun, C. Jeong, J. Heo, N. J. Kim, *Angewandte Chemie-International Edition* **2014**, *53*, 7805-7808.

[14] A. Hong, C. J. Moon, H. Jang, A. Min, M. Y. Choi, J. Heo, N. J. Kim, *Journal of Physical Chemistry Letters* **2018**, *9*, 476-480.

[15] H. Ganjitabar, R. Hadidi, G. A. Garcia, L. Nahon, I. Powis, *Journal of Molecular Spectroscopy* **2018**, *353*, 11-19.

[16] L. Nahon, L. Nag, G. A. Garcia, I. Myrgorodska, U. Meierhenrich, S. Beaulieu, V. Wanie, V. Blanchet, R. Geneaux, I. Powis, *Physical Chemistry Chemical Physics* **2016**, *18*, 12696-12706.

[17] S. Turchini, *Journal of Physics-Condensed Matter* **2017**, *29*, 503001.

[18] S. Daly, M. Tia, G. A. Garcia, L. Nahon, I. Powis, *Angewandte Chemie-International Edition* **2016**, *55*, 11054-11058.

[19] R. Hadidi, D. K. Božanić, H. Ganjitabar, G. A. Garcia, I. Powis, L. Nahon, *Communications Chemistry* **2021**, *4*, 72.

[20] J. Dupont, V. Lepere, A. Zehnacker, S. Hartweg, G. A. Garcia, L. Nahon, *The Journal of Physical Chemistry letters* **2022**, *13*, 2313-2320.

[21] I. Powis, in *Advances in Chemical Physics, Vol 138, Vol. 138* (Ed.: S. A. Rice), **2008**, pp. 267-329.

[22] L. Nahon, G. A. Garcia, I. Powis, *Journal of Electron Spectroscopy and Related Phenomena* **2015**, *204*, 322-334.

[23] R. Hadidi, D. K. Bozanic, G. A. Garcia, L. Nahon, *Advances in Physics-X* **2018**, *3*, 833-861.

[24] A. Giardini, D. Catone, S. Stranges, M. Satta, M. Tacconi, S. Piccirillo, S. Turchini, N. Zema, G. Contini, T. Prosperi, P. Decleva, D. Di Tommaso, G. Fronzoni, M. Stener, A. Filippi, M. Speranza, *ChemPhysChem* **2005**, *6*, 1164-1168.

[25] G. A. Garcia, L. Nahon, C. J. Harding, I. Powis, *Physical Chemistry Chemical Physics* **2008**, *10*, 1628-1639.

[26] S. Turchini, D. Catone, G. Contini, N. Zema, S. Irrera, M. Stener, D. Di Tommaso, P. Decleva, T. Prosperi, *ChemPhysChem* **2009**, *10*, 1839-1846.

[27] G. A. Garcia, H. Soldi-Lose, L. Nahon, I. Powis, *Journal of Physical Chemistry A* **2010**, *114*, 847-853.

[28] S. Turchini, D. Catone, N. Zema, G. Contini, T. Prosperi, P. Decleva, M. Stener, F. Rondino, S. Piccirillo, K. C. Prince, M. Speranza, *ChemPhysChem* **2013**, *14*, 1723-1732.

[29] M. Tia, B. C. de Miranda, S. Daly, F. Gaie-Levrel, G. A. Garcia, L. Nahon, I. Powis, *Journal of Physical Chemistry A* **2014**, *118*, 2765-2779.

[30] D. Catone, S. Turchini, G. Contini, T. Prosperi, M. Stener, P. Decleva, N. Zema, *Chemical Physics* **2017**, *482*, 294-302.

[31] S. Hartweg, G. A. Garcia, D. K. Bozanic, L. Nahon, *Journal of Physical Chemistry Letters* **2021**, *12*, 2385-2393.

[32] J. Triptow, A. Fielicke, G. Meijer, M. Green, *Angewandte Chemie-International Edition* **2023**, *62*, e202212020.

[33] C. J. Harding, E. Mikajlo, I. Powis, S. Barth, S. Joshi, V. Ulrich, U. Hergenhahn, *Journal of Chemical Physics* **2005**, *123*.

[34] I. Powis, C. J. Harding, S. Barth, S. Joshi, V. Ulrich, U. Hergenhahn, *Physical Review A* **2008**, *78*.

[35] C. Lux, M. Wollenhaupt, T. Bolze, Q. Liang, J. Koehler, C. Sarpe, T. Baumert, *Angewandte Chemie-International Edition* **2012**, *51*, 5001-5005.

[36] C. S. Lehmann, N. B. Ram, I. Powis, M. H. M. Janssen, *Journal of Chemical Physics* **2013**, *139*, 234307.

[37] M. M. R. Fanood, I. Powis, M. H. M. Janssen, *Journal of Physical Chemistry A* **2014**, *118*, 11541-11546.

[38] C. Lux, M. Wollenhaupt, C. Sarpe, T. Baumert, *ChemPhysChem* **2015**, *16*, 115-137.

[39] A. Comby, S. Beaulieu, M. Boggio-Pasqua, D. Descamps, F. Legare, L. Nahon, S. Petit, B. Pons, B. Fabre, Y. Mairesse, V. Blanchett, *Journal of Physical Chemistry Letters* **2016**, *7*, 4514-4519.

[40] V. Blanchet, D. Descamps, S. Petit, Y. Mairesse, B. Pons, B. Fabre, *Physical Chemistry Chemical Physics* **2021**, *23*, 25612-25628.

[41] A. Kastner, T. Ring, B. C. Kruger, G. B. Park, T. Schafer, A. Senftleben, T. Baumert, *Journal of Chemical Physics* **2017**, *147*.

[42] A. Kastner, G. Koumarianou, P. Glodic, P. Samartzis, N. Ladda, S. T. Ranecky, T. Ring, V. Sudheendran, C. Witte, H. Braun, H. G. Lee, A. Senftleben, R. Berger, G. B. Park, T. Schafer, T. Baumert, *Physical Chemistry Chemical Physics* **2020**, *22*, 7404-7411.

[43] S. T. Ranecky, G. B. Park, P. C. Samartzis, I. C. Giannakidis, D. Schwarzer, A. Senftleben, T. Baumert, T. Schaefer, *Physical Chemistry Chemical Physics* **2022**, *24*, 2758-2761.

[44] F. BenNasr, A. Pérez-Mellor, I. Alata, V. Lepere, N. E. Jaidane, A. Zehnacker, *Faraday Discussions* **2018**, *212*, 399-419.

[45] J. Altnoeder, A. Bouchet, J. J. Lee, K. E. Otto, M. A. Suhm, A. Zehnacker-Rentien, *Physical Chemistry Chemical Physics* **2013**, *15*, 10167-10180.

[46] A. Bouchet, J. Altnoder, M. Broquier, A. Zehnacker, *Journal of Molecular Structure* **2014**, *1076*, 344-351.

[47] D. Scuderi, A. Paladini, M. Satta, D. Catone, S. Piccirillo, M. Speranza, A. G. Guidoni, *Physical Chemistry Chemical Physics* **2002**, *4*, 4999-5003.

[48] K. Le Barbu-Debus, F. Lahmani, A. Zehnacker-Rentien, N. Guchhait, S. S. Panja, T. Chakraborty, *Journal of Chemical Physics* **2006**, *125*, 174305.

[49] B. Velino, P. Ottaviani, W. Caminati, A. Giardini, A. Paladini, *ChemPhysChem* **2006**, *7*, 565-568.

[50] A. O. Hernandez-Castillo, J. Bischoff, J. H. Lee, J. Langenhan, M. Karra, G. Meijer, S. Eibenberger-Arias, *Physical Chemistry Chemical Physics* **2021**, *23*, 7048-7056.

[51] J. Lee, J. Bischoff, A. O. Hernandez-Castillo, B. Sartakov, G. Meijer, S. Eibenberger-Arias, *Physical Review Letters* **2022**, *128*.

[52] I. Powis, *Journal of Chemical Physics* **2014**, *140*.

[53] G. A. Garcia, L. Nahon, S. Daly, I. Powis, *Nature Communications* **2013**, *4*, 2132.

[54] H. Ganjitabar, G. A. Garcia, L. Nahon, I. Powis, *Journal of Chemical Physics* **2020**, *153*, 034302.

[55] S. Beaulieu, A. Comby, B. Fabre, D. Descamps, A. Ferre, G. Garcia, R. Geneaux, F. Legare, L. Nahon, S. Petit, T. Ruchon, B. Pons, V. Blanchet, Y. Mairesse, *Faraday Discussions* **2016**, *194*, 325-348.

[56] L. Wunsch, F. Metz, H. J. Neusser, E. W. Schlag, *Journal of Chemical Physics* **1977**, *66*, 386-400.

[57] S.-h. Urashima, M. Miyazaki, M. Fujii, H. Saigusa, *Chemistry Letters* **2013**, *42*, 1070-1072.

[58] E. H. Van Kleef, I. Powis, *Molecular Physics* **1999**, *96*, 757-774.

[59] C. Jeong, J. Yun, J. Heo, N. J. Kim, *Physical Chemistry Chemical Physics* **2023**.

[60] M. H. M. Janssen, I. Powis, *Physical Chemistry Chemical Physics* **2014**, *16*, 856-871.

[61] K. Le Barbu-Debus, M. Broquier, A. Mahjoub, A. Zehnacker-Rentien, *Physical Chemistry Chemical Physics* **2009**, *11*, 7589-7598.

[62] D. Scuderi, K. Le Barbu-Debus, A. Zehnacker, *Physical Chemistry Chemical Physics* **2011**, *13*, 17916-17929.

[63] M. Albrecht, A. Borba, K. Le Barbu-Debus, B. Dittrich, R. Fausto, S. Grimme, A. Mahjoub, M. Nedic, U. Schmitt, L. Schrader, M. A. Suhm, A. Zehnacker-Rentien, J. Zischang, *New Journal of Chemistry* **2010**, *34*, 1266-1285.
[64] A. Kastner, C. Lux, T. Ring, S. Zullighoven, C. Sarpe, A. Senftleben, T. Baumert, *ChemPhysChem* **2016**, *17*, 1119-1122.
[65] M. H. M. Janssen, I. Powis, *Spectroscopy on line* **2017**, *15*, 16-23.
[66] A. Comby, D. Descamps, S. Petit, E. Valzer, M. Wloch, L. Pouysegu, S. Quideau, J. Bockova, C. Meinert, V. Blanchet, B. Fabre, Y. Mairesse, *Physical Chemistry Chemical Physics* **2023**, *25*, 16246-16263.
[67] M. M. R. Fanood, N. B. Ram, C. S. Lehmann, I. Powis, M. H. M. Janssen, *Nature Communications* **2015**, *6*, 7511-.
[68] A. Comby, E. Bloch, C. M. M. Bond, D. Descamps, J. Miles, S. Petit, S. Rozen, J. B. Greenwood, V. Blanchet, Y. Mairesse, *Nature Communications* **2018**, *9*, 5212.
[69] C. A. Taatjes, O. Welz, A. J. Eskola, J. D. Savee, A. M. Scheer, D. E. Shallcross, B. Rotavera, E. P. F. Lee, J. M. Dyke, D. K. W. Mok, D. L. Osborn, C. J. Percival, *Science* **2013**, *340*, 177-180.
[70] N. Seurre, K. Le Barbu-Debus, F. Lahmani, A. Zehnacker, N. Borho, M. A. Suhm, *Physical Chemistry Chemical Physics* **2006**, *8*, 1007-1016.
[71] N. Seurre, J. Sepiol, K. Le Barbu-Debus, F. Lahmani, A. Zehnacker-Rentien, *Physical Chemistry Chemical Physics* **2004**, *6*, 2867-2877.
[72] B. Hartwig, M. Lange, A. Poblotzki, R. Medel, A. Zehnacker, M. A. Suhm, *Physical Chemistry Chemical Physics* **2020**, *22*, 1122-1136.
[73] A. R. AlRabaa, K. Le Barbu, F. Lahmani, A. Zehnacker-Rentien, *Journal of Photochemistry and Photobiology A-Chemistry* **1997**, *105*, 277-282.
[74] A. AlRabaa, K. Le Barbu, F. Lahmani, A. Zehnacker-Rentien, *Journal of Physical Chemistry A* **1997**, *101*, 3273-3278.
[75] N. Borho, T. Haber, M. A. Suhm, *Physical Chemistry Chemical Physics* **2001**, *3*, 1945-1948.
[76] N. Borho, M. A. Suhm, *Physical Chemistry Chemical Physics* **2002**, *4*, 2721-2732.
[77] N. Borho, M. A. Suhm, *Organic & Biomolecular Chemistry* **2003**, *1*, 4351-4358.
[78] T. B. Adler, N. Borho, M. Reiher, M. A. Suhm, *Angewandte Chemie-International Edition* **2006**, *45*, 3440-3445.
[79] A. Filippi, A. Giardini, A. Latini, S. Piccirillo, D. Scuderi, M. Speranza, *International Journal of Mass Spectrometry* **2001**, *210*, 483-488.
[80] D. Scuderi, A. Paladini, M. Satta, D. Catone, F. Rondino, M. Tacconi, A. Filippi, S. Piccirillo, A. Giardini-Guidoni, M. Speranza, *Physical Chemistry Chemical Physics* **2003**, *5*, 4570-4575.

Table of Contents

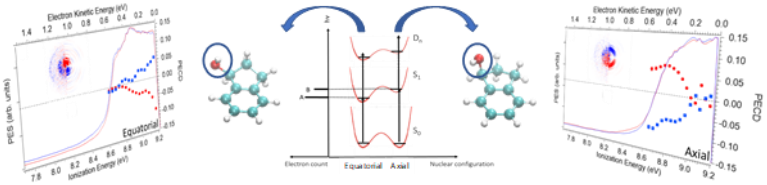

Conformer selective Photoelectron Circular Dichroism of chiral 1-indanol is obtained via a resonance-enhanced two-photon ionization scheme, thanks to the selectivity due to the $S_1 \leftarrow S_0$ transition. The equatorial and axial conformers of 1-indanol display PECD that dramatically differ in both amplitude and sign.

SUPPLEMENTARY INFORMATION

Experimental Methods

Commercially-available samples of enantiopure 1-indanol were purchased from Sigma-Aldrich for the (*S*)-(+) enantiomer and Biosynth Carbosynth for the (*R*)-(-) enantiomer. A pulsed supersonic beam was produced by expanding 2 bar of helium through a 200 μm pulsed nozzle (General Valve – Parker, 10 Hz), [1] seeded with 1-indanol brought into the gas phase by resistive heating in an oven at 55 °C. Mass-resolved electronic spectra were obtained using one-color resonance-enhanced two-photon ionization (RE2PI) as reported previously and were shown to be identical to that recorded by monitoring the electrons.[2] The UV source was a frequency-doubled dye laser (Sirah equipped with C540A dye) pumped by the second harmonic of a Nd:YAG laser (Surelite III – Continuum, repetition rate: 10 Hz). It crossed at right angle the skimmed supersonic beam (skimmer of 500 μm diameter) between two grids-less electrodes separated by 9 mm, as schematically depicted in Figure 1 of the main text. The light source providing the second photon for recording the two-photon 2-color spectra was a counter-propagating OPO system (Continuum Surelite II + Optical Parametric Oscillator, Horizon system, repetition rate: 10 Hz, pulse-duration: 4 ns, spectral width 5 cm^{-1}). The excitation and ionization lasers were synchronized in time by a homemade controller. The alignment of the ionizing laser was checked by recording the 1C-R2PI PECD obtained by setting this laser on the transition origin. We have optimized the power of the two lasers to minimize the contribution of signal induced by the second photon alone. The total electron signal was averaged by an oscilloscope (Lecroy wavesurfer) and processed through a personal computer to monitor the UV spectrum. The electrons were accelerated and analyzed by a velocity map imaging (VMI) spectrometer designed by Photek and coupled to a CCD camera (IDS Imaging UI-3060CP-M-GL Rev.2).

12 to 24 successive files of 5 million counts each were recorded with alternating right and left light helicity for each selected transition of 1-indanol. The corresponding raw electron images were processed with Abel-inversion via the pBasex software.[3] The pBasex software is based on the Abel transform of the electron distribution and aims to reconstruct the three-dimensional Newton sphere of the expanding electrons from its two-dimensional projection. It consists of fitting a set of polar basis functions with a known and exact inverse Abel function. The sum (LCP+RPC) image provided the PES and the PECD was defined as the relative difference in electron counts through the backward and forward hemispheres, resulting to PECD = $2b_1$-$0.5b_3$.[4-5] The electronic densities were calculated at the MP2 level of theory using the Gaussian software, version G16 B01.[6] The isodensity of the HOMO was plotted with the VMD software, with an isodensity value of 0.04.[7] The energy of the HOMO was reported previously and was calculated with the outer valence Green's function (OVGF) method and cc-pVTZ basis set.[8-10]

Structure and vibrational frequencies of the (S)-1-indanol conformers

Table S1: Structure of the I_{eq} conformer in the neutral ground state optimized at the B3LYP-D3BJ /6-311G++(d,p) level (xyz file - coordinates in Å).

C	0.0693590000	-0.4064490000	0.1860840000
C	-0.3418300000	0.9237020000	0.0366370000
C	-1.6931160000	1.2260720000	-0.1272820000
C	-2.6251020000	0.1818320000	-0.1427380000
C	-2.2100090000	-1.1470960000	0.0078110000
C	-0.8547700000	-1.4497170000	0.1786960000
H	-2.0207490000	2.2550680000	-0.2497600000
H	-3.6796510000	0.4034460000	-0.2779850000
H	-2.9452030000	-1.9460970000	-0.0093470000
H	-0.5228350000	-2.4775450000	0.2938010000
C	1.5734210000	-0.4834610000	0.3570770000
H	1.8285660000	-0.6179950000	1.4157830000
C	0.8505090000	1.8555410000	0.0993820000
H	0.9179320000	2.3190460000	1.0931160000
H	0.7971080000	2.6706980000	-0.6295090000
C	2.0474070000	0.9040810000	-0.1413360000
H	2.2410980000	0.8255100000	-1.2188520000
H	2.9734580000	1.2301590000	0.3386200000
O	2.1947930000	-1.5907940000	-0.2899120000
H	1.9221300000	-1.5874610000	-1.2185600000

Table S2: Structure of the II_{ax} conformer in the neutral ground state optimized at the B3LYP-D3BJ /6-311G++(d,p) level (xyz file - coordinates in Å).

C	-0.0269120000	-0.4816930000	-0.2284240000
C	0.2283840000	0.8666300000	0.0597960000
C	1.5373270000	1.3026110000	0.2565980000
C	2.5853580000	0.3787740000	0.1583930000
C	2.3282420000	-0.9650710000	-0.1347430000
C	1.0132510000	-1.4037210000	-0.3303910000
H	1.7477980000	2.3459350000	0.4758610000
H	3.6095830000	0.7102640000	0.3019240000
H	3.1525120000	-1.6667330000	-0.2196220000
H	0.8125890000	-2.4451960000	-0.5707470000
C	-1.5171000000	-0.7204810000	-0.3403420000
H	-1.7812120000	-1.4175050000	-1.1468230000
C	-1.0650740000	1.6502390000	0.1079270000
H	-0.9942210000	2.6182510000	-0.3984410000
H	-1.3506530000	1.8468210000	1.1486670000
C	-2.0760570000	0.6935170000	-0.5728230000
H	-3.0933380000	0.7801800000	-0.1838860000
H	-2.1011070000	0.8915630000	-1.6500990000
O	-2.0686050000	-1.2064510000	0.9012490000
H	-1.4949810000	-1.9065790000	1.2395440000

Table S3: Vibrational frequencies of the I_{eq} conformer in the ionic state calculated at the B3LYP-D3BJ /6-311G++(d,p) level (not scaled)

Frequency (cm^{-1})	Intensity ($km.mol^{-1}$)	
105.2	2.1	
142.9	**1.1**	**Puckering motion** 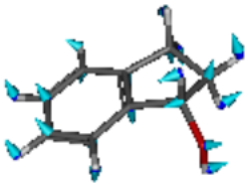
200.2	2.3	
240.1	8.6	
294.1	50.9	
358.8	1	
404.8	2.6	
430.9	13.6	
470.3	6.6	
481.2	6.4	
542.6	11.1	
595.4	6.4	
664.5	1.1	
739.9	6.9	
776.9	46.1	
805.9	5.6	
832.6	5	
887.4	7.2	
949.8	7.1	
958.3	55.4	
976.7	15.2	
987.5	24.4	
996.2	6	
1012.1	0.2	
1093.7	61.8	
1106.1	35.6	
1119	1.9	
1150.1	181.9	
1179	35.8	
1195.3	7.5	
1217.9	14.7	
1240.7	39.7	
1251.9	6.7	
1267.7	19.1	
1320.9	9.7	
1338.5	6.2	
1384.6	**68.5**	**Coupled β(OH)/ β(OH) bends** 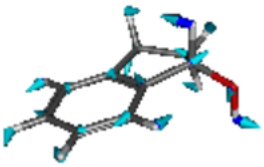
1396.8	3	
1410.5	78.4	
1470.4	24.7	
1478.6	119.4	
1500	4.4	
1519	5.5	
1563.7	86.4	
2989.7	7.5	

2992	24.7
3069.2	21
3077.4	3.9
3164.5	1.9
3211.9	0
3218.5	0.8
3226.5	4.5
3230.3	1.6
3785.1	**101.1**

ν(OH) stretching mode

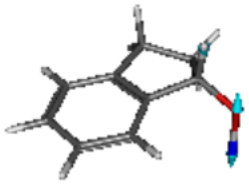

Table S4: Vibrational frequencies of the II_{ax} conformer in the ionic state calculated at the B3LYP-D3BJ/6-311G++(d,p) level (not scaled).

Frequency (cm^{-1})	Intensity ($km.mol^{-1}$)
103.3	1
124.7	**4.1**
186.3	29.7
242.9	38.5
325.6	72.6
351.4	61
404.6	4.5
426.6	34.9
436.6	15.6
534.3	2.2
561.7	21.9
640.7	5.2
717.5	8.9
764.1	26.1
782.9	29
832	5.7
843.4	50.8
876.4	1
898.7	4
942.1	22.8
987.3	6.5
991.2	22.1
1004.1	18.6
1014.4	0.4
1036.1	5.7
1121.1	61.6
1124.2	13.9
1138.5	12
1188.6	9.5
1194.7	8.4
1214.1	30
1234	5
1263.9	10.7

Puckering motion

1302.9	6.6	
1330.1	7.2	
1349	16.3	
1371.3	**21.3**	**Coupled β(OH)/ β(OH) bends**
1408.8	3.2	
1426.2	69.2	
1479.2	36.7	
1480.3	64.7	
1490.2	72.2	
1524.6	3.7	
1567.3	60.5	
3009.6	26.1	
3086.4	4.2	
3100.4	0.2	
3120	16	
3155.2	0.1	
3210.4	0.1	
3215.4	0.4	
3223.7	2.1	
3228.8	0.6	
3785.8	**219.8**	**ν(OH) stretching mode**

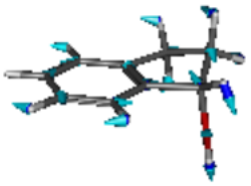

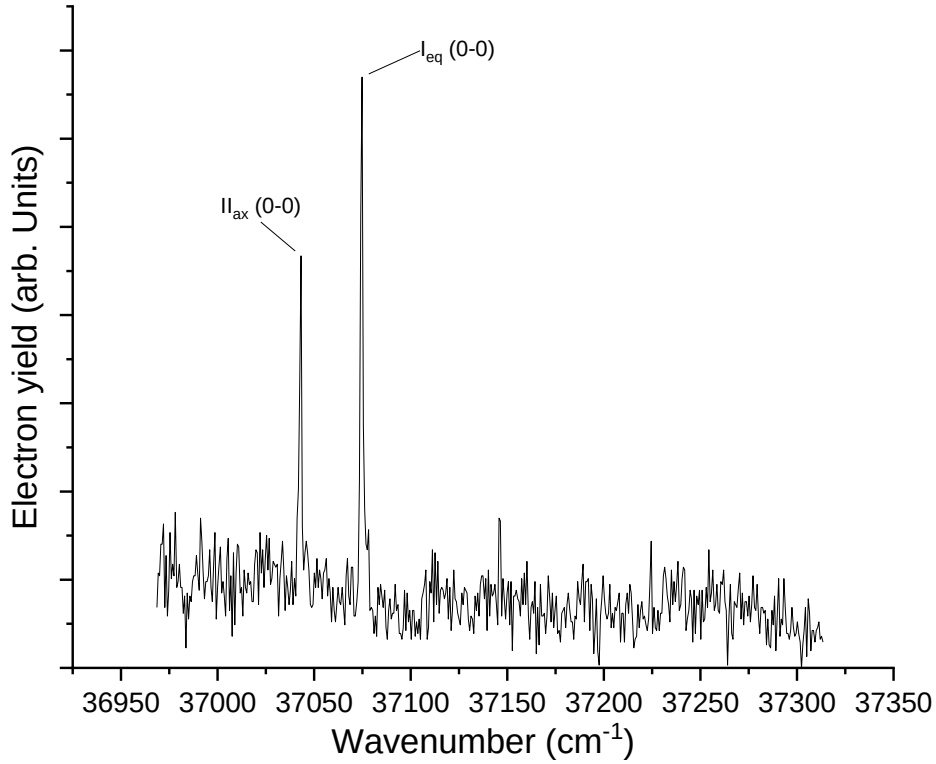

Figure S1: two-color $S_1 \leftarrow S_0$ spectrum obtained by monitoring the total number of electrons as a function of the excitation laser wavenumber. The ionization laser is fixed at 40000 cm^{-1}.

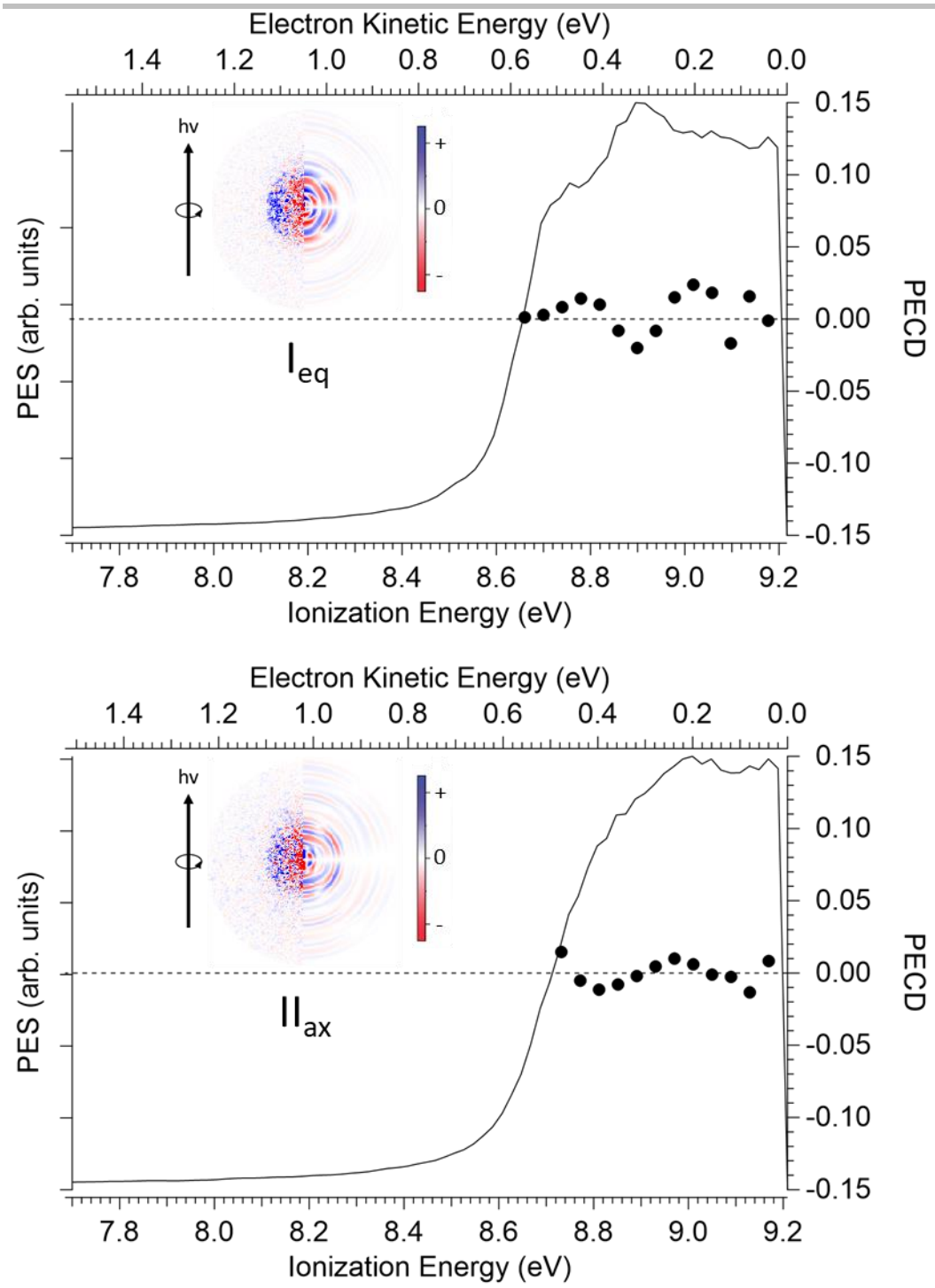

Figure S2: a) Photoelectron spectra (full line) and PECD (squares) of racemic 1-indanol excited at the equatorial (I_{eq}) transition origin at 37075 cm^{-1} (total ionization energy of 9.1976 eV) in a one-color scheme. b) Same for the axial conformer (II_{ax}) excited at its transition origin at 37043 cm^{-1} (total ionization energy of 9.1897 eV). The inserts are the LCP-RCP raw (left) and Abel inverted (right) electron images for both conformers.

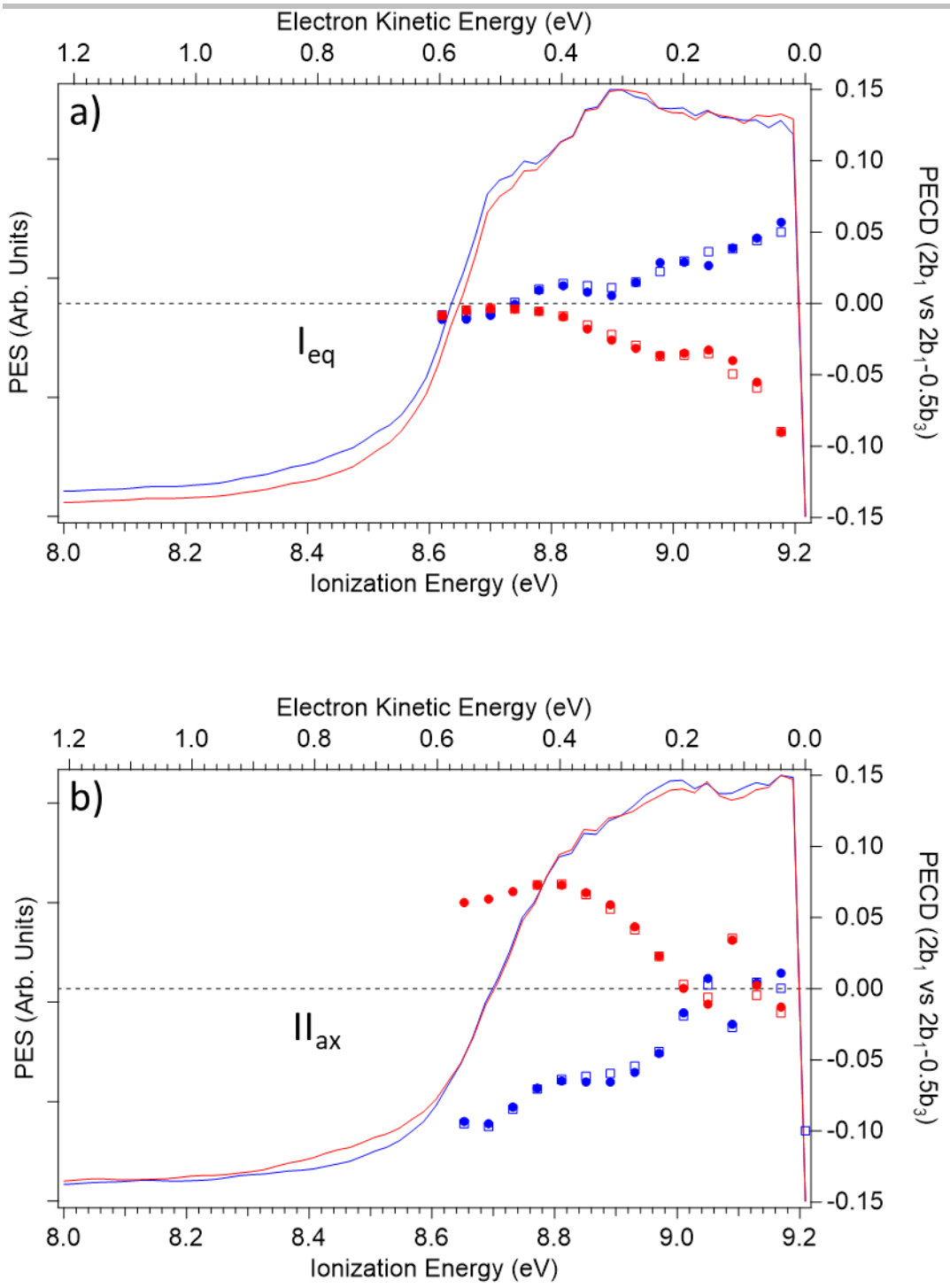

Figure S3: a) Photoelectron spectra (full line) and PECD (squares) for the two enantiomers of 1-indanol excited at the equatorial transition origin at 37075 cm^{-1} (total ionization energy of 9.1976 eV) in a one-color scheme. b) Same for the axial conformer excited at its transition origin at 37043 cm^{-1} (total ionization energy of 9.1897 eV). The (*R*) enantiomer is shown in blue and the (*S*) in red. The full symbols correspond to $2b_1 - 0.5b_3$ and the empty symbols correspond to $2b_1$

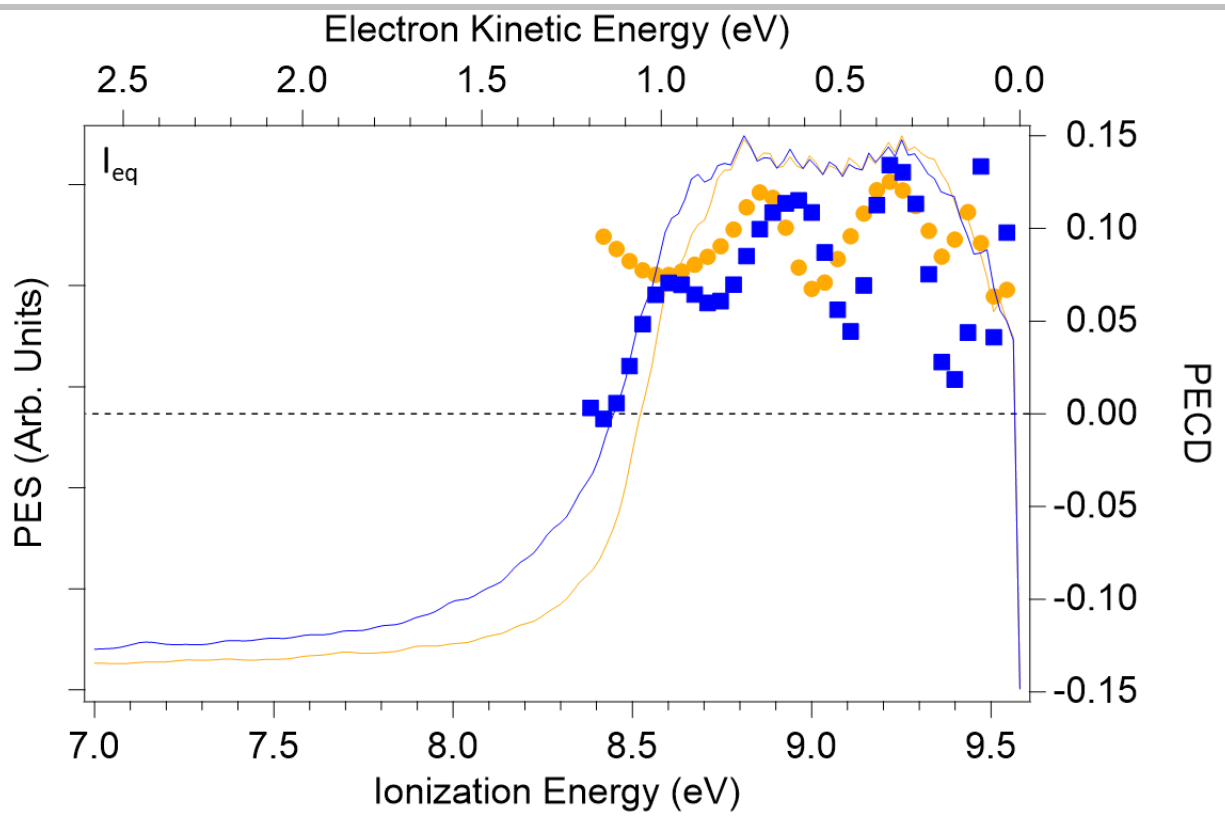

Figure S4: Two-color photoelectron spectra (full line) and PECD (squares) for (*R*) 1-indanol excited at the equatorial (I_{eq}) transition origin at 37075 cm^{-1}. The energy of the ionizing laser is 40000 cm^{-1}. The polarization of the excitation laser is circular (blue) in a parallel scheme or linear vertical (orange).

REFERENCES

[S1] D. Scuderi, K. Le Barbu-Debus, A. Zehnacker, *Physical Chemistry Chemical Physics* **2011**, *13*, 17916-17929.
[S2] F. BenNasr, A. Pérez-Mellor, I. Alata, V. Lepere, N. E. Jaidane, A. Zehnacker, *Faraday Discussions* **2018**, *212*, 399-419.
[S3] G. A. Garcia, L. Nahon, I. Powis, *Review of Scientific Instruments* **2004**, *75*, 4989-4996.
[S4] L. Nahon, G. A. Garcia, C. J. Harding, E. Mikajlo, I. Powis, *Journal of Chemical Physics* **2006**, *125*, 114309-.
[S5] C. S. Lehmann, N. B. Ram, I. Powis, M. H. M. Janssen, *Journal of Chemical Physics* **2013**, *139*, 234307.
[S6] M. J. Frisch, G. W. Trucks, H. B. Schlegel, G. E. Scuseria, M. A. Robb, J. R. Cheeseman, G. Scalmani, V. Barone, G. A. Petersson, H. Nakatsuji, X. Li, M. Caricato, A. V. Marenich, J. Bloino, B. G. Janesko, R. Gomperts, B. Mennucci, H. P. Hratchian, J. V. Ortiz, A. F. Izmaylov, J. L. Sonnenberg, Williams, F. Ding, F. Lipparini, F. Egidi, J. Goings, B. Peng, A. Petrone, T. Henderson, D. Ranasinghe, V. G. Zakrzewski, J. Gao, N. Rega, G. Zheng, W. Liang, M. Hada, M. Ehara, K. Toyota, R. Fukuda, J. Hasegawa, M. Ishida, T. Nakajima, Y. Honda, O. Kitao, H. Nakai, T. Vreven, K. Throssell, J. A. Montgomery Jr., J. E. Peralta, F. Ogliaro, M. J. Bearpark, J. J. Heyd, E. N. Brothers, K. N. Kudin, V. N. Staroverov, T. A. Keith, R. Kobayashi, J. Normand, K. Raghavachari, A. P. Rendell, J. C. Burant, S. S. Iyengar, J. Tomasi, M. Cossi, J. M. Millam, M. Klene, C. Adamo, R. Cammi, J. W. Ochterski, R. L. Martin, K. Morokuma, O. Farkas, J. B. Foresman, D. J. Fox, Wallingford, CT, **2016**.
[S7] W. Humphrey, A. Dalke, K. Schulten, *J. Molec. Graphics* **1996**, *14*, 33-38.
[S8] W. Vonniessen, J. Schirmer, L. S. Cederbaum, *Computer Physics Reports* **1984**, *1*, 57-125.
[S9] G. A. Garcia, L. Nahon, C. J. Harding, I. Powis, *Physical Chemistry Chemical Physics* **2008**, *10*, 1628-1639.
[S10] J. Dupont, V. Lepere, A. Zehnacker, S. Hartweg, G. A. Garcia, L. Nahon, *The Journal of Physical Chemistry letters* **2022**, *13*, 2313-2320.